Page Proof Instructions and Queries

Thank you for choosing to publish with us. This is your final opportunity to ensure your article will be accurate at publication. Please review your proof carefully and respond to the queries using the circled tools in the image below, which are available **by clicking "Comment"** from the right-side menu in Adobe Reader DC.*

Please use *only* the tools circled in the image, as edits via other tools/methods can be lost during file conversion. For comments, questions, or formatting requests, please use [T]. Please do *not* use comment bubbles/sticky notes ⊙.

*If you do not see these tools, please ensure you have opened this file with **Adobe Reader DC**, available for free at get.adobe.com/reader or by going to Help > Check for Updates within other versions of Reader. For more detailed instructions, please see us.sagepub.com/ReaderXProofs.

Sl. No.	Query
	Please note, only ORCID iDs validated prior to acceptance will be authorized for publication; we are unable to add or amend ORCID iDs at this stage.
	Please confirm that all author information, including names, affiliations, sequence, and contact details, is correct.
	Please review the entire document for typographical errors, mathematical errors, and any other necessary corrections; check headings, tables, and figures.
	Please ensure that you have obtained and enclosed all necessary permissions for the reproduction of art works (e.g. illustrations, photographs, charts, maps, other visual material, etc.) not owned by yourself. Please refer to your publishing agreement for further information.
	Please note that this proof represents your final opportunity to review your article prior to publication, so please do send all of your changes now.
	Please confirm that the Acknowledgment, Funding and Conflict of Interest statements are accurate.
1	Please check the sentence 'The specimens were manufactured …' for clarity.
2	Please check whether the hierarchy of section heading levels is correct throughout the article.
3	Please check whether all citations are correct as given in all instances.
4	Please check whether all abbreviations/acronyms and its expansions are correct as given in all instances.
5	Throughout the article, please check whether the figure, table, section and equation citations refer to the correct figures, tables, sections and equations.
6	Please check whether Figures 1 to 10 are correct as set.
7	Please check whether the captions of all figures and tables are correct as given.
8	Please check the sentence 'The stiffness of this bearing …' for clarity.
9	Please check the sentence 'We considered as design variables …' for clarity.
10	Please check whether Tables 1 and 2 are correct as set.
11	Please check whether the column and row heads are correct as given in Tables 1 and 2.
12	Please check whether the values and units are correct as given in all instances.
13	Please check whether the edits made to the sentence 'Figure 3(a) and (b) shows the …' and the following sentence are correct.
14	Please check the sentence 'Figure 6 shows the half-normal …' and the following sentence for clarity.
15	' R. Mead, S. G. Gilmour, 2012' has been changed to 'Mead et al., 2012' to match with the reference list. Please check.
16	Please check the sentence 'The models were automatically …' for clarity.
17	Please check whether variables/terms/functions/Greeks are accurately and consistently used in all instances.

18   Please check whether all the equations are correct as set.
19   Please check the sentence 'The influence of the anisotropy of …' for clarity.

Magneto-mechanical characterization of magnetorheological elastomers

Alberto Bellelli and Andrea Spaggiari 🆔

Abstract
This work analyses the properties and the magneto-mechanical characteristics of magnetorheological elastomers, a class of smart materials not yet broadly investigated. First, set of several samples of this material was manufactured, each one characterized by a different percentage of ferromagnetic material inside the viscoelastic matrix. The specimens were manufactured in order to create isotropic and anisotropic configurations, respectively, with randomly dispersed ferromagnetic particles or with an aligned distribution, obtained through and external magnetic field.[AQ: 1] Then, the mechanical behaviour of each sample was analysed by conducting a compression test, both with and without an external magnetic field. Moreover, a three-point bending test was also performed on the same specimens. Stiffness, deformation at maximum stress and specific energy dissipated were calculated based on the experimental data. The results were analysed considering the mechanical responses, and an analysis of variance was carried out in order to assess the statistical influence of each variable. The experimental results highlighted a strong correlation between the percentage of ferromagnetic material in each sample and its mechanical behaviour. The anisotropicity of the material, aligned in columnar structures, also affects the stiffness measured in the compression test, while the external magnetic field's main contribution is to reduce the samples' maximum deformation. Using analysis of variance results as guidelines, we built a simple phenomenological model which produces quite reliable predictions regarding the mechanical response of the magnetorheological elastomers under compressive stress.

Keywords
magnetorheological, magnetorheology, elastomers, experimental tests, analysis of variance

1. Introduction[AQ: 2]

The study of magnetorheological elastomers (MREs), materials whose properties are still an open research field, since their use is still limited to some niche applications, was born from the curiosity towards a viscoelastic material mainly sold as a toy, Silly Putty (Cross, 2012; Hartzman, 2013), especially in its magnetic sensitive form (Golinelli et al., 2015). Silly Putty is probably one of the best examples of a viscoelastic material, because it is incredibly stiff in case of high deformation rates, while it is very deformable and soft for quasi-static applied stress (Cross, 2012). This semi-fluid behaviour makes Silly Putty unsuitable for engineering applications, since it cannot keep a desired shape, and it also collapses under its own weight, which is unacceptable for many applications. The natural development to obtain more interesting performances is to study MREs, which consist of ferromagnetic micrometric particles suspended in a non-magnetic elastomeric matrix (Davis, 1999; Guan et al., 2008; Ruddy et al., 2008) and, quite opposite to Silly Putty, they do

not exhibit a fluid-like behaviour. The magnetic interactions between the particles in these composite materials depend on the magnetic orientation of each particle and their spatial relationship, which leads to an interesting number of magneto-mechanical phenomena (De Vicente et al., 2011; Ginder et al., 2000; Kallio, 2005). The aim is to expand the applicability of MREs towards the more widespread field of magnetorheological fluids (MRFs) which exploit the same principle using a fluid matrix and are already used in many industrial applications, especially for vibration damping and shock absorbers (Carlson and Jolly, 2000; Chen et al., 2007; Shen et al., 2004; Spaggiari et al., 2016; Yang et al., 2015).[AQ: 3][AQ: 4]

Department of Sciences and Methods for Engineering, University of Modena and Reggio Emilia, Reggio Emilia, Italy

Corresponding author:
Andrea Spaggiari, Department of Sciences and Methods for Engineering, University of Modena and Reggio Emilia, Reggio Emilia 42122, Italy.
Email: andrea.spaggiari@unimore.it

MREs include a large variety of composite materials, but their main components are always ferromagnetic particles immersed in a non-magnetic elastomeric matrix. The constituents of MREs, the technologies for their manufacture and the mathematical models that best describe their mechanical properties present a range of very interesting scientific problems that are only partially treated in the scientific literature (Chen et al., 2007). Compared to MRFs, MREs always show a solid behaviour, that is, they do not pass from fluid to quasi-solid state; however, their mechanical characteristics in terms of stiffness and damping are a function not only of the external mechanical loads, but also of the applied external magnetic field. Moreover, the change of the macroscopic properties of MREs is quite limited compared to MRFs but MREs are much more manageable than MRFs, which have the problems of confinement and compatibility with standard gaskets and can easily be damaged by the friction with magnetic particles (Güth et al., 2013; Spaggiari and Dragoni, 2012; Wiehe and Maas, 2012). One of the most important characteristics which make MREs different form MRFs is the possibility to obtain both isotropic and anisotropic configurations during the manufacturing of the samples, which is not possible with MRFs. The ferromagnetic particles within the elastomeric matrix can be homogeneously distributed forming isotropic MREs during the matrix cure, as shown in Figure 1(a), or they can be forced to form chain-like column structures, forming anisotropic MREs as shown in Figure 1(b) due to the application of an external magnetic field.[AQ: 5]

The external magnetic field applied to the MRE induces dipolar moments in the ferromagnetic particles before the complete polymerization of the elastomer, so that the columnar structures of particles remain locked in place until the end of the cure, and then this structure is fixed in the matrix. MREs have a potential use especially in the design of simple devices with variable stiffness and good controllability (Han et al., 2013; Southern, 2008). Ford Motor Company has patented a bearing for automotive applications including the use of a MRE. The stiffness of this bearing is adjusted according to the state in which the powertrain is, in order to optimize the suspension thus improving passengers' comfort.[AQ: 8] It may be noted that although to date a number of applications that involve the use of anisotropic MREs have been patented, no industrial product is yet available on the market, probably since their performance still does not justify their costs. This article investigates a MRE made by a peculiar elastomeric matrix, which shows a quite versatile behaviour as it can be cast in various shapes, undergoes large deformations and opens interesting possibilities to exploit it as smart sensor.

2. Materials and methods

The manufacture of the specimens was carried out following a design of experiment procedure (Montgomery, 2004). We considered as design variables five different weight fractions of ferromagnetic particles, the isotropicity of the specimens and the application of an external magnetic field.[AQ: 9] For each configuration, we manufactured two samples for a total of 18 specimens. Subsequently, we carried out compression tests, with or without an external magnetic field and three-point bending tests.

2.1 Experimental apparatus

The elastomeric matrix was obtained from a commercial polydimethylsiloxane (PDMS) base, Sylgard 184 (Dow Corning Sylgard 184 TDS Krayden, 2013), which is a two-component material which is widely used in electronic applications, especially for encapsulation of microelectronics circuits. This material shows very interesting properties as an electret (Kachroudi et al., 2017) and it was already described and studied in Kachroudi et al. (2015), where its viscoelastic, thermal and dielectric properties can be found. The aim of this article is to study and discuss its magnetorheological properties when enriched by various weight fractions of ferromagnetic particles. The elastomeric base was mixed with carbonyl iron particles with an average size of 45 μm – Ferchim RI 63/3.2 by Pometon (Metal granules production iron powders supplier – POMETON POWDER, n.d.). The three ingredients (curing agent, silicone base and iron powder), after being weighted to obtain the desired weight fraction, were deposited and mixed in a plastic mould designed to obtain the desired specimens. The specimens' dimensions were 60 × 30 × 10 mm, with a slight draft angle to improve the extraction of the polymerized elastomer. The mould was equipped with a top cover of the same material. Since manual mixing of the components always introduced air inside the mould, the top cover was equipped with a set of holes which allowed gas extraction, obtained using a vacuum chamber at
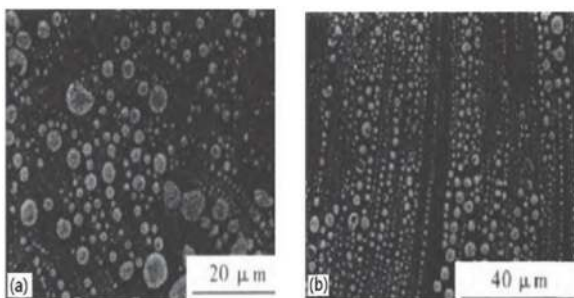

Figure 1.[AQ: 6] Microscopic structure of an MRE: (a) isotropic MRE and (b) anisotropic MRE (Lian et al., 2015).[AQ: 7]
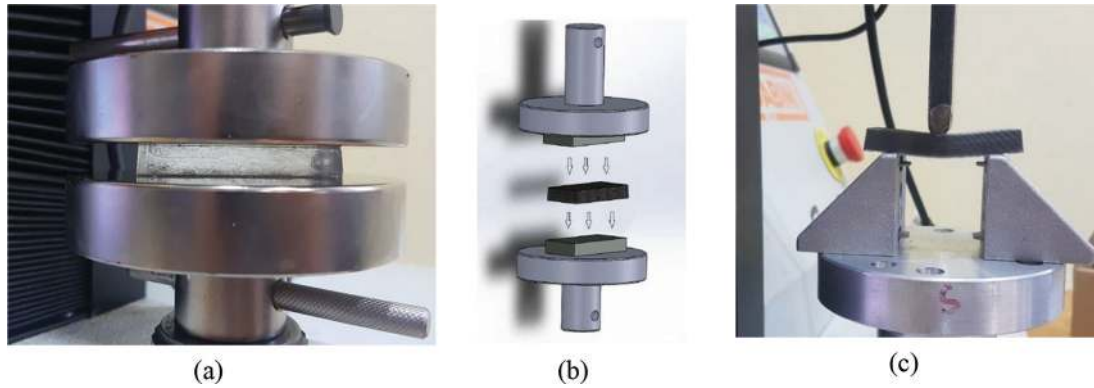
Figure 2. Compression test without magnets on pure elastomer specimen (a), compression test scheme with permanent magnets (b) and three-point bending test setup (c).

Table 1.[AQ: 10] Specimens considered in the design plan.[AQ: 11]

Variable	Number of levels	Specimens								
% Ferromagnetic material	5 levels	0	20		40		60		80	
Isotropicity	Boolean	N/A	YES	NO	YES	NO	YES	NO	YES	NO
Replicates	2	2	2		2		2		2	
Total specimens	18	2	4		4		4		4	

−0.8 bar. The mould, containing the reagents still in the liquid phase, was left for 15 min in the vacuum chamber to ensure a proper elimination of air bubbles and then the curing step started. The mould was placed in slow rotation through a stepper motor in order to avoid the settling of the iron particles due to the gravity and it was kept for 6 h in a climatic chamber at 45°C to ensure the complete polymerization of the elastomeric matrix. A total of 18 specimens were manufactured according to the previously described procedure. First, the eight isotropic specimens were obtained, with different percentages by weight of ferromagnetic material (20%, 40%, 60%, 80%), two samples for each fraction considered. In order to produce the other eight anisotropic specimens, a couple of permanent magnets were placed around the mould when the system was still uncured. The effect of the magnetic field led to the formation of an aligned arrangement of particles inside the specimens. The magnetic induction field provided by the magnets, measured experimentally through a Gaussmeter (in air), was around 200 mT, enough to obtain particle movement and chain formation. In the end, the last two control specimens of pure PDMS, with no ferromagnetic particles, were manufactured to estimate the base material properties under the same test conditions of the magnetorheological samples. The specimens were tested under compression tests and under three-point bending tests, as described in Figure 2. The tensile test was not taken into consideration because the grippers would have caused severe stress concentrations, which undermine the test results, and in addition, the elastomers do not perform well under tensile stresses. Both the compression and the bending tests were non-destructive since we decided to limit the test to the elastic properties of the material and no plasticization is expected for a hyper elastic material. The desired test conditions were ensured by limiting the maximum force to 400 N in compression tests and limiting the maximum deflection to 2 mm in three-point bending tests. These limit values were calibrated after a set of preliminary tests, not reported here for the sake of brevity. The tests were quasi-static, and a single loading/unloading curve was recorded at a speed of 1 mm/min. The experimental plan included the execution of the compression and the three-point bending tests on 18 specimens. Table 1 reports a synthetic representation of the variables considered.

2.1.1 Compression test rig. The compression test exploited two steel plates mounted on the base and on the head of the test machine, a Galdabini Sun 500, equipped with a 5000 N load cell, as shown in Figure 6(a). The tests performed were 36: each of the 18 specimens was tested both in the absence and in the presence of an external magnetic field. The external magnetic field was again obtained with two permanent magnets providing a quite uniform distribution around 200 mT (Figure 6(b)). In order to estimate a possible effect of the magnetic force due to the permanent magnets, we carried
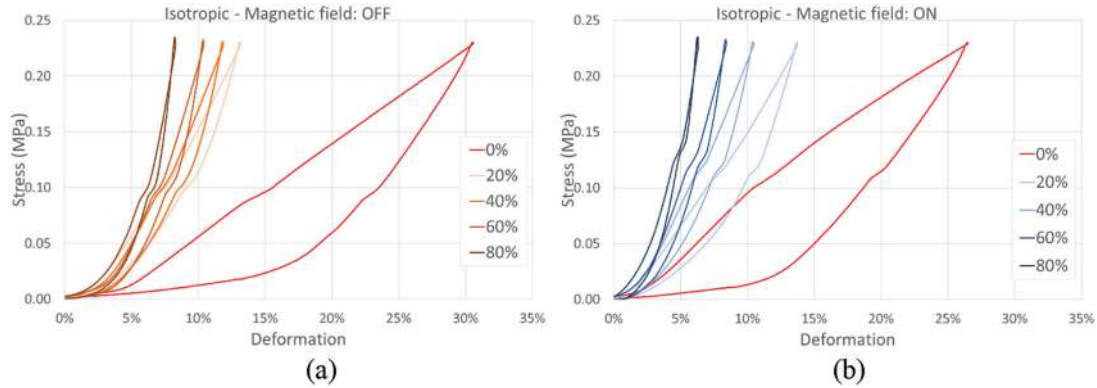
Figure 3. Compression test on isotropic specimens, without (a) and with the field applied (b).
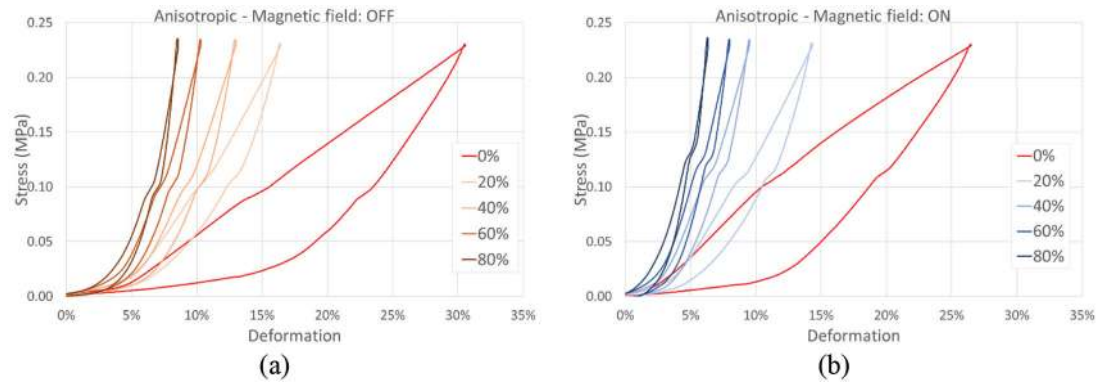

Figure 4. Compression test on anisotropic specimens, without (a) and with the magnetic field applied (b).

out several test with magnets only, but a maximum force of about 3 N was measured, far from the 400 N and therefore negligible. The responses of the system were obtained from the load–displacement curves by computing the following quantities:

- Stiffness, computed as the slope of the first elastic part of the stress–strain curves (MPa).
- Strain, measured at maximum applied load of 400 N (%).[AQ: 12]
- Specific dissipated energy (mJ/mm^3), that is, the area between the loading and unloading curve.

2.1.2 Three-point bending test rig. The first important difference between the compression test and the three-point bending test is that we decided to eliminate the external magnetic field from the set of variables, since the punch position would have disturbed the magnetic system. The specimen dimensions were the same used in the compression tests, as well as the test responses. The bending stiffness was derived by the force displacement curves according to the classic Timoshenko beam theory. The test involved the use of two fixed supports with a distance of 40 mm, and a central punch was used

to apply a 2 mm displacement at 1 mm/min speed at the centre of the system. To increase the sensibility of the test rig, the machine was equipped with a smaller 250 N load cell. No stabilization of the samples with cyclic loading was provided before the test execution, both under compression and bending.

3. Experimental results

Figure 3(a) and (b) shows the curves σ–ε for isotropic specimens without the applied field and with the field applied during the compression test, respectively. [AQ: 13]Figure 4(a) and (b) shows the curves for the anisotropic specimens without the applied field and with the field applied during the compression test, respectively, while Figure 5 shows the curves for the three-point bending specimens, isotropic and anisotropic, with no magnetic field applied.

The Payne effect (Clément et al., 2005) and the Mullin effect (Wang et al., 2015), which are quite typical for PDMS matrix with fillers, were not taken into account in the model, since the deformations are not large enough to trigger the Mullin effect and the tests are quasi-static, thus the change in the storage modulus
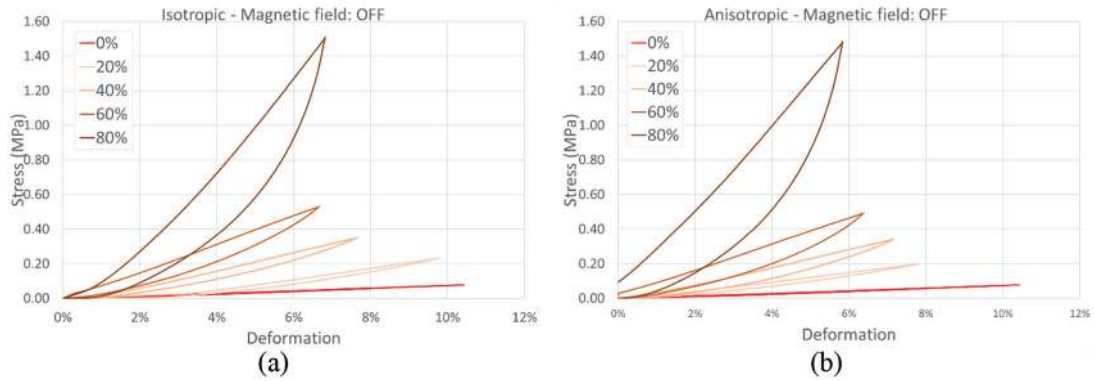
Figure 5. Three-point bending test on isotropic (a) and anisotropic specimens (b).
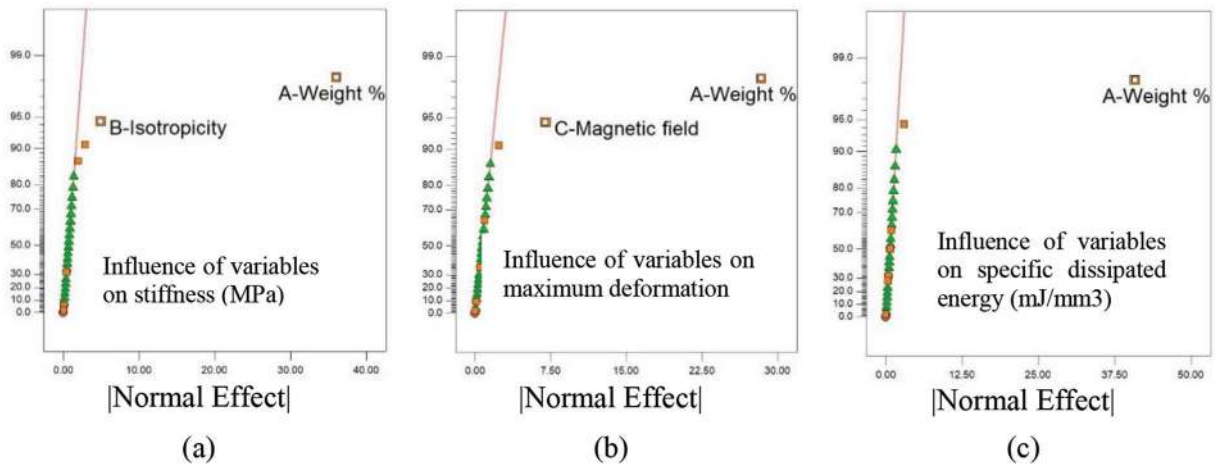

Figure 6. Half-normal diagrams concerning the analysis of stiffness (a), maximum deformation (b) and specific energy dissipated (c) in compression tests.

typical of the Payne effect is limited and therefore negligible.

4. Discussion

The experimental tests were analysed by evaluating the response of the material in terms of stiffness, strain at maximum stress and dissipated energy, as described in Section 3. A statistical software, Stat-Ease Design-Expert (Anderson and Whitcomb, 2007), was used to verify the influence and interactions of the variables considered. The results were analysed according to the variable plan shown in Table 1. Figure 6 shows the half-normal diagrams of the three responses considered (Mead, 1990; Mead et al., 2012), useful for estimating the variables that have an influence on the response at a glance.[AQ: 14] The stronger the influence, the larger the distance from the error line, extrapolated from the green triangles, which represent the normal stochastic variation of an experimental test.[AQ: 15]

Figure 6 diagrams show the variables that have a statistically significant influence on the response of the specimen. This influence is greater as they deviate from the error bar and the X-axis represents the influence on the response while the Y-axis the confidence that the effect is not due to experimental noise. Figure 7 shows the effect of the ferromagnetic particles on the responses. Figure 7(a) shows that the stiffness increases as the particles' concentration increases, while the anisotropicity causes only a slight increase in stiffness. Figure 7(b) shows the effect of the reinforcement content on the maximum deformation and the weak effect of the applied field, which reduces the maximum deformation of the material due to the additional restraint of the particles affected by the applied field: the ferromagnetic particles are more constrained under the effect of compression, so the behaviour is more rigid. Figure 7(c) shows the effect of the particles content on the dissipated energy, which, as shown in Figure 6(c), is not influenced by the applied field or the isotropicity of the specimen.
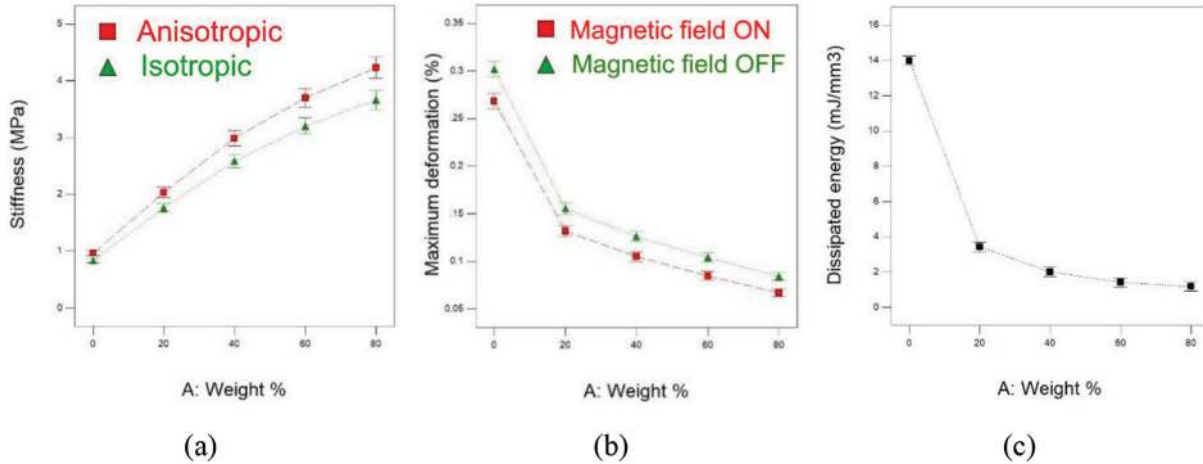
Figure 7. Compression tests. Stiffness as a function of alignment and percentage of particles (a). Maximum deformation as a function of applied magnetic field and percentage of particles (b). Energy dissipated as a function of percentage of particles (c).
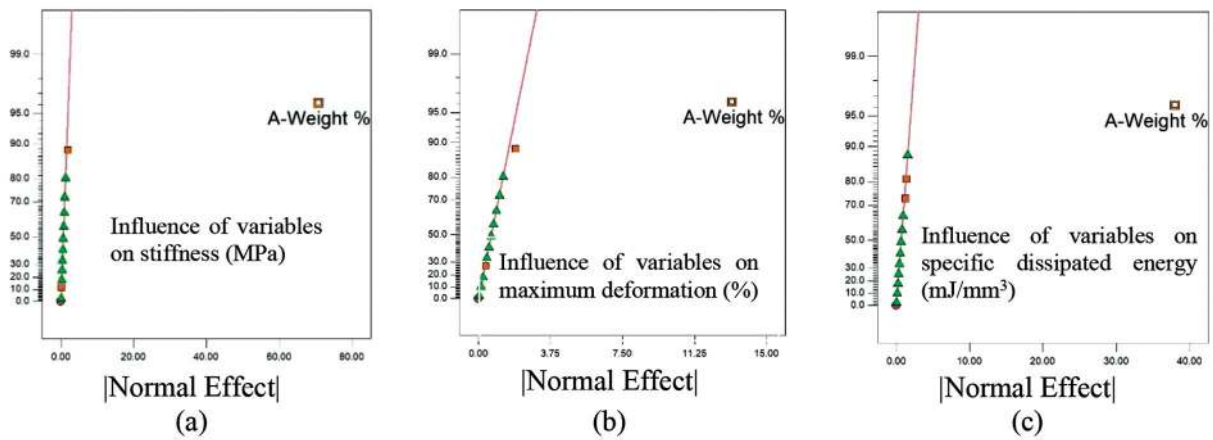

Figure 8. Half-normal diagrams of the three-point bending tests for stiffness (a), maximum deformation (b) and specific energy dissipated (c). No transformation applied.

The analysis of variance (ANOVA) was carried out in the three-point bending tests as well, according to the experimental plan described in the previous paragraphs, considering the same responses of the compression tests. The half-normal diagrams of the three considered responses are shown in Figure 8.

It was convenient, also in this case, to represent the behaviour of the MREs in three-point bending as a function of the ferromagnetic particles only. In particular, in Figure 9(a), we note that the stiffness increases as the iron concentration increases, above all there is a slight increase up to 60% and a very high increase from 60% to 80%. Figure 9(b) shows the effect of the reinforcement content on maximum deformation: the reinforcement content reduces the maximum deformation of the material, as for the compressive tests.

Figure 9(c) shows the effect of the reinforcement content on the dissipated energy, which, as shown by

the ANOVA, is influenced only by the amount of particles present in the elastomer. The weight fraction of ferromagnetic particles increases the energy dissipated in a very strong way between 60% and 80%, with an opposite trend compared to Figure 7(c). The alignment in columnar structures of ferromagnetic particles does not affect the response of the system. In compression tests, an influence of the alignment of the specimens was more likely to occur, since they were stressed in the same direction as the columnar structures, while in the bending stress it is possible to imagine that this type of anisotropicity is almost irrelevant. The difference in orientation of the ferromagnetic particles with respect to the loading direction could be a motivation for the different behaviour of the compressive tests and the bending tests, especially at 80%. Even though the statistical analysis does not highlight any effect of the isotropicity of the material in general, the 80% specimens
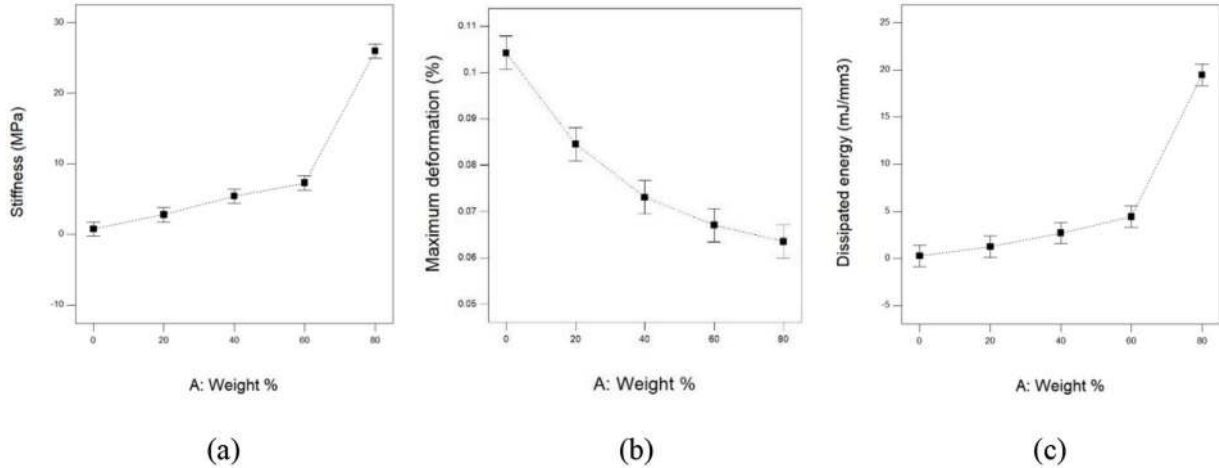
Figure 9. Bending tests. Stiffness as a function of percentage of particles (a). Maximum deformation as a function of percentage of particles (b). Energy dissipated as a function of percentage of particles (c). No transformation applied.

Table 2. ANOVA summary table.

	Compression			Three-point bending	
	Increase in % weight	Anisotropicity	Magnetic field presence	Increase in % weight	Anisotropicity
Stiffness (MPa)	↑↑↑	↑↑	↑	↑↑	x
Maximum deformation (%)	↓↓↓	x	↓↓	↓↓	x
Dissipated energy (mJ/mm³)	↓↓	x	x	↑↑	x

ANOVA: analysis of variance.

show a very sharp increase of the dissipated energy in bending. This increase could be motivated by the influence of the loading direction: when compressed, the columnar structures will provide a direct support for the load, while in case of bending the columns of particles are not capable to provide a support, the PDMS matrix carries the vast majority of the load and therefore a more dissipative behaviour is provided.

Table 2 reports an ANOVA summary table showing the influence of each individual factor on the analysed responses of the system. The results are consistent with the findings of other researchers (Kukla et al., 2017; Schrittesser et al., 2009) which are based on a physical based parameters, such as storage modulus and loss modulus, but both confirms the stiffening effect of the ferromagnetic particles especially at high weight fractions.

The stiffening of the material due to the particles could be modelled with a power law, as shown in Figure 7(a), but we did not perform and inverse analysis of the results, since we wanted to exploit the ANOVA data to provide a simpler model. The predictive models were obtained for each response of the system. The detailed description of just one of these is reported below for the sake of brevity, while the models are

expressed in equation (1) for the stiffness, expressed in MPa, in equation (2) for the maximum deformation (%) and in equation (3) for the dissipated energy, expressed in mJ/mm³. The models were automatically generated by the ANOVA software used, Stat-Ease Design-Expert.[AQ: 16] The software linearizes the responses and to do so it applies a so-called transformation whenever useful as for the stiffness (natural log) and for the maximum strain (root square). The expressions above are reported for coded factors, a compact form used to express the levels of the variables considered. Figure 10(a) shows the graphical meaning of the four coded factors $A[i]$ considered, which are used to represent all the possible levels of ferromagnetic particles. The other variables are much simpler to be used, B is the isotropicity (isotropic $\rightarrow B = 1$, anisotropic $\rightarrow B = -1$) and C is the magnetic field applied (field ON $\rightarrow C = -1$, field OFF $\rightarrow C = 1$).Once the desired configuration is chosen, the prediction can be done. The comparison of the prediction and the model is reported in Figure 10(b), with the model (Y-axis) and the experimental results (X-axis) for the natural logarithm of the stiffness in compression. The agreement seems quite good, considering the simple phenomenological model adopted[AQ: 17]
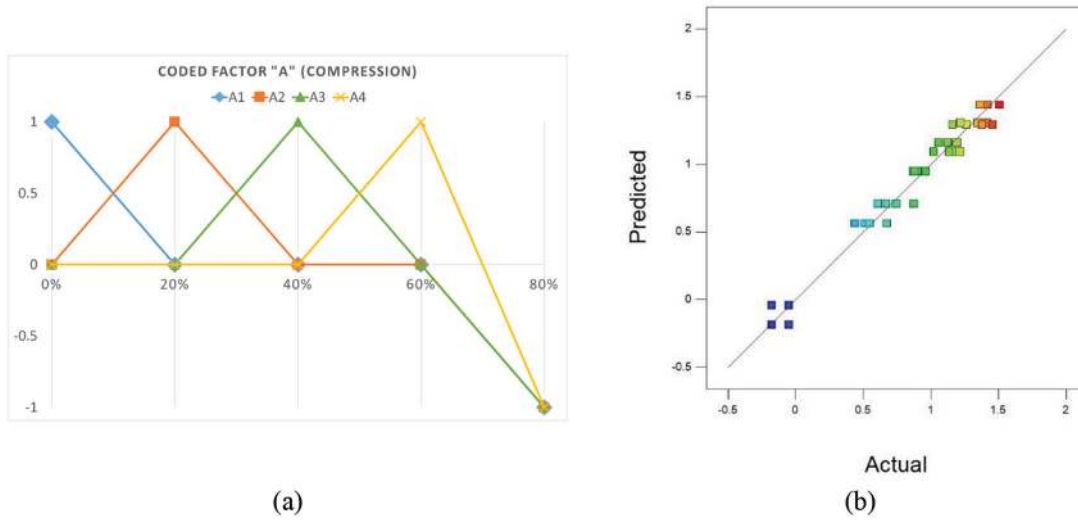
Figure 10. Coded factors (a) and accuracy of the proposed model of stiffness (compression) in terms of prediction and experimental points (b).

$$Ln(Stiffness) = 0.83 - 0.94 \cdot A[1] - 0.19 \cdot A[2] \\ + 0.19 \cdot A[3] + 0.40 \cdot A[4] - 0.072 \cdot B \\ - 0.038 \cdot C \tag{1}$$

$$Sqrt(Max. deformation) = 0.37 + 0.17 \cdot A[1] + 0.012 \cdot A[2] \\ - 0.027 \cdot A[3] - 0.060 \cdot A[4] \\ + 0.016 \cdot C \tag{2}$$

[AQ: 18]
$$Dissipated\ energy = 4.41 + 9.58 \cdot A[1] - 0.98 \cdot A[2] \\ - 2.39 \cdot A[3] - 2.99 \cdot A[4] \tag{3}$$

It is immediate to understand that only the dissipated energy shows a linear dependence on the ferromagnetic particles: the stiffness shows a logarithmic increase and the maximum deformation shows a quadratic decrease with the increase of the reinforce.

An example on how to exploit the provided models is reported for the sake of clarity. The hypothesis is that one would like to predict the stiffness in compression of an anisotropic 50% specimen without magnetic field applied. The equations provided would give the following result

$$Ln(Stiffness) = 0.83 - 0.94 \cdot 0 - 0.19 \cdot 0 + 0.19 \cdot 0.5 \\ + 0.40 \cdot 0.5 - 0.072 \cdot (-1) - 0.038 \cdot 1 \\ = 1.159 \tag{4}$$

$$Stiffness = e^{1.159} \approx 3.19\,\mathrm{MPa} \tag{5}$$

5. Conclusion

This work analyses the magneto-mechanical behaviour of a MRE in compression and bending. The experimental tests show that the weight fraction of ferromagnetic material present in the viscoelastic matrix strongly affects the MRE behaviour. In compression, the stiffness of the specimens, with other factors being equal, shows an important increase with the larger ferromagnetic particles weight fraction. In bending tests, a strong non-linearity of the behaviour is found. Up to 60% of ferromagnetic weight fraction, there is a slight increase in stiffness, while the 80% specimens show a peak in stiffness increment. The deformation at maximum stress, on the other hand, decreases as the percentage of ferromagnetic material increases. This applies to both compression tests and bending tests. The specific energy dissipated in compression decreases with the increase in the percentage of ferromagnetic material. Conversely, under three-point bending, the behaviour is quite the opposite, since a strong increase is found especially for the 80% weight fraction specimen. The physical motivation of this discrepancy will be further investigated with specific tests. The influence of the anisotropy of the particles created ad hoc during the polymerization is not high for the bending tests, while in compression tests, the anisotropic specimens show higher stiffness values than isotropic specimens.[AQ: 19] The alignment of the particles, on the other hand, does not influence either the maximum deformation or the specific energy dissipated. Deformation at maximum stress is the response most influenced by the external magnetic field, even though the most important variable which controls the specimen behaviour is always the weight fraction of ferromagnetic particles. The application of the

magnetic field shows a decrease in the maximum deformation, while there is no influence of the field on the dissipated energy. This is probably due to the fact that the field strength has to be higher to modify the material behaviour, considering the PDMS natural stiffness.

Acknowledgements

Declaration of conflicting interests

Funding

ORCID iD

Andrea Spaggiari https://orcid.org/0000-0001-8959-2599

References

Anderson MJ and Whitcomb PJ (2007) *DOE Simplified: Practical Tools for Effective Experimentation*. 2nd ed. New York: Productivity Press.

Carlson JD and Jolly MR (2000) MR fluid, foam and elastomer devices. *Mechatronics* 10(4–5): 555–569.

Chen L, Gong XL and Li WH (2007) Microstructures and viscoelastic properties of anisotropic magnetorheological elastomers. *Smart Materials and Structures* 16(6): 2645–2650.

Clément F, Bokobza L and Monnerie L (2005) Investigation of the Payne effect and its temperature dependence on silica-filled polydimethylsiloxane networks: part I: experimental results. *Rubber Chemistry and Technology* 78(2): 211–231.

Cross R (2012) Elastic and viscous properties of Silly Putty. *American Journal of Physics* 80(10): 870–875.

Davis LC (1999) Model of magnetorheological elastomers. *Journal of Applied Physics* 85(6): 3348.

De Vicente J, Klingenberg DJ and Hidalgo-Alvarez R (2011) Magnetorheological fluids: a review. *Soft Matter* 7(8): 3701.

Dow Corning Sylgard 184 TDS Krayden (2013). Available at: https://krayden.com/technical-data-sheet/dow_corning_sylgard_184_technical_data_sheet/ (accessed 13 September 2018).

Ginder JM, Nichols ME, Elie LD, et al. (2000) Controllable-stiffness components based on magnetorheological elastomers. In: *SPIE's 7th annual international symposium on smart structures and materials*, vol. 3985, Newport Beach, CA, 6–9 March, pp. 418–425. Bellingham, WA: SPIE.

Golinelli N, Spaggiari A and Dragoni E (2015) Mechanical behaviour of magnetic Silly Putty: viscoelastic and magnetorheological properties. *Journal of Intelligent Material Systems and Structures* 28(8): 953–960.

Guan X, Dong X and Ou J (2008) Magnetostrictive effect of magnetorheological elastomer. *Journal of Magnetism and Magnetic Materials* 320(3–4): 158–163.

Güth D, Wiebe A, Maas J, et al. (2013) Design of shear gaps for high-speed and high-load MRF brakes and clutches. *Journal of Physics: Conference Series* 412(1): 012046.

Han Y, Hong W and Faidley LE (2013) Field-stiffening effect of magneto-rheological elastomers. *International Journal of Solids and Structures* 50(14–15): 2281–2288.

Hartzman M (2013) A touch of knowledge: the very serious history of Silly Putty. *HuffPost*. Available at: https://www.huffingtonpost.com/marc-hartzman/a-touch-of-knowledge-the-_2_b_1308405.html?guccounter = 1 (accessed 13 September 2018).

Kachroudi A, Basrour S and Sylvestre A (2017) Thermal stability of micro-structured PDMS piezo-electrets under various polymeric reticulation ratios for sensor applications. *Proceedings* 1(4): 310.

Kachroudi A, Basrour S, Rufer L, et al. (2015) Piezoelectric cellular micro-structured PDMS material for micro-sensors and energy harvesting. *Journal of Physics: Conference Series* 660(1): 012040.

Kallio M (2005) *The elastic and damping properties of magnetorheological elastomers*. PhD Thesis, VTT Technical Research Centre of Finland, Espoo.

Kukla M, Górecki J, Malujda I, et al. (2017) The determination of mechanical properties of magnetorheological elastomers (MREs). *Procedia Engineering* 177: 324–330.

Lian C, Lee K-H and Lee C-H (2015) Friction and wear characterics of magneto-rheological elastomers based on silicone/polyurethane hybrid. *Journal of Tribology* 137(3): 031607.

Mead R (1990) *The Design of Experiments: Statistical Principles for Practical Applications*. Cambridge: Cambridge University Press. Available at: https://books.google.com/books?hl = it&lr = &id = CaFZPbCllrMC&pgis = 1 (accessed 3 November 2015).

Mead R, Gilmour SG and Mead A (2012) *Statistical Principles for the Design of Experiments: Applications to Real Experiments*. Cambridge: Cambridge University Press. Available at: http://www.amazon.com/Statistical-Principles-Design-Experiments-Probabilistic/dp/0521862140 (accessed 3 November 2015).

Metal granules production iron powders supplier – POMETON POWDER (n.d.). Available at: http://www.pometon.com/materialsScheda_eng.php/prodotto = selefer/id_prod = 17/from = search (accessed 13 September 2018).

Montgomery DC (2004) *Design and Analysis of Experiments*. Hoboken, NJ: John Wiley & Sons.

Ruddy C, Ahearne E and Byrne G (2008) A review of magnetorheological elastomers: properties and applications. Available at: http://www.ucd.ie/mecheng/ams/news_items/CillianRuddy.pdf (accessed 8 March 2017).

Schrittesser B, Major Z and Filipcsei G (2009) Characterization of the dynamic mechanical behavior of magneto – elastomers. *Journal of Physics: Conference Series* 149: 012096.

Shen Y, Golnaraghi MF and Heppler GR (2004) Experimental research and modeling of magnetorheological

elastomers. *Journal of Intelligent Material Systems and Structures* 15(1): 27–35.

Southern BM (2008) *Design and characterization of tunable magneto-rheological fluid-elastic mounts*. Master's Thesis, Virginia Tech, Blacksburg, VA.

Spaggiari A and Dragoni E (2012) Efficient dynamic modelling and characterization of a magnetorheological damper. *Meccanica* 47(8): 2041–2054.

Spaggiari A, Castagnetti D, Golinelli N, et al. (2016) Smart materials: properties, design and mechatronic applications. *Proceedings of the Institution of Mechanical Engineers, Part L: Journal of Materials: Design and Applications.* Epub ahead of print 12 December. DOI: 10.1177/1464420716673671.

Wang Z, Li S, Wei D, et al. (2015) Mechanical properties, Payne effect, and Mullins effect of thermoplastic vulcanizates based on high-impact polystyrene and styrene–butadiene rubber compatibilized by styrene–butadiene–styrene block copolymer. *Journal of Thermoplastic Composite Materials* 28(8): 1154–1172.

Wiehe A and Maas J (2012) Large-scale test bench for the durability analysis of magnetorheological fluids. *Journal of Intelligent Material Systems and Structures* 24(12): 1433–1444.

Yang C, Fu J, Yu M, et al. (2015) A new magnetorheological elastomer isolator in shear–compression mixed mode. *Journal of Intelligent Material Systems and Structures* 26(10): 1290–1300.